Paper CIT02-0125

HYDRODYNAMIC STABILITY IN AN ELECTROCHEMICAL CELL WITH ROTATING DISK ELECTRODE

J. Pontes
Metallurgy and Materials Engineering Department – EE/COPPE/UFRJ
PO Box 68505, 21945-970 Rio de Janeiro RJ, Brazil
jopontes@.ufrj.br

Norberto Mangiavacchi
Institute of Mathematical and Computational Sciences USP – S. Carlos,
PO Box 668, 13560-161 S.Carlos, SP, Brazil
norberto@icmc.sc.usp.br

Anderson R. Conceição
Metallurgy and Materials Engineering Department – EE/UFRJ
PO Box 68505, 21945-970 Rio de Janeiro RJ, Brazil
anderson@metalmat.ufrj.br

Oswaldo E. Barcia
Institute of Chemistry – UFRJ,
PO Box 68505, 21945-970 Rio de Janeiro, Brazil
barcia@metalmat.ufrj.br

Oscar Rosa Mattos
Metallurgy and Materials Engineering Department – COPPE/UFRJ
PO Box 68505, 21945-970 Rio de Janeiro RJ, Brazil
omattos@metalmat.ufrj.br

Bernard Tribollet
UPR15 – CNRS, Physique des Liquides et Electrochimie,
4 place Jussieu, 75252 Paris Cedex 05, France
bt@ccr.jussieu.fr

Abstract. Polarization curves experimentally obtained in the electro-dissolution of iron in a 1 **M** $\mathbf{H_2SO_4}$ solution using a rotating disk as the working electrode present a current instability region within the range of applied voltage in which the current is controlled by mass transport in the electrolyte. According to the literature (Barcia et. al., 1992) the electrodissolution process leads to the existence of a viscosity gradient in the interface metal-solution. The viscosity gradient changes the velocity field and may affect the stability properties of the steady flow developed close to the rotating disk electrode. On a previous paper, Pontes et. al. (2002) showed that this is indeed the case when the steady flow is perturbed by disturbances with periodic variation along the radial direction. In this paper we extend those results by considering the linear stability of the flow with respect to perturbations with periodic variation along the radial and azimutal directions. It is shown that the neutral stability curves are modified by the presence of a viscosity gradient, in the sense of reducing the critical Reynolds number beyond which perturbations are amplified. Comparison with the results obtained by Malik (1986) for constant viscosity fluids show good agreement. The results presented suport the hypothesis that the current oscillations observed in the polarization curve may originate from a hydrodynamic instability.

Keywords: *Rotating Disk Flow, Eletrochemical Instabilities, Hydrodynamic Stability, Turbulence*

1. Introduction

Polarization curves experimentally obtained in the electro-dissolution of iron in a 1 **M** $\mathbf{H_2SO_4}$ solution using a rotating disk as the working electrode present three different regions (Barcia et. al., 1992). The first region is associated with low overvoltages applied to the working electrode and the current is a function of the electric potential and dissolution process only. The electric current is controlled by the transfer of charges at the interface rotating disk/electrolyte solution, and the mass transport does not affect the electro-dissolution process.

By increasing the the applied potential, the curves show a second region where the hydrodynamic conditions, which depend on the angular velocity imposed to the rotating disk electrode, affect the rate of the anodic dissolution of iron. The current is a function both of the applied potential and the hydrodynamic field developed close to the rotating electrode. By further increasing the applied overvoltage a third region appears, where the current is totally controlled by mass-transport processes. In this third region, polarization curves present a current plateau, defining a limit value for the current, which depends on the hydrodynamic conditions set by the angular velocity of the electrode.

Two current instabilities are observed in the third region: one at the beginning of the current plateau and a second one at the end, where the electrode surface undergoes an active to passive transition (Ferreira et. al., 1994). The first instability is intrinsic to the system, while the current instability close to the active-passive transition is affected by the output impedance of the control equipment. This instability can be supressed by using a negative feedback resistance (Epelboin, 1972), that gives rise to a continuous curves. Barcia et. al. (1992) proposed that the electro-dissolution process leads to the existence of a viscosity gradient in the diffusion boundary layer, which modifies the steady velocity field close to the electrode and could affect the stability of the hydrodynamic field. On a previous paper, Pontes et. al. (2002) showed that this is indeed the case when the steady rotating disk flow is perturbed by disturbances with periodic variation along the radial direction. The base state was assumed as the classical rotating disk flow (Von Kármán, 1921 Schlichting, 1968), modified by the existence of a viscosity gradient pointing along the axial direction. In this paper we extend those results by considering the stability of the flow with respect to perturbations with periodic variation along the radial and azimutal directions. The results are compared with those presented by Malik (1996), Faller (1991) and Lingwood (1996).

For a review of the literature concerning current instabilities in electrochemical cells and in rotating disk flow of fluids with constant viscosity, the reader is referred to the paper by Pontes et. al. (2002).

The paper is organized as follows: Section (2) describes the steady velocity flow, which is the problem base state, for the case of constant viscosity fluids and for six viscosity profiles configurations assumed in this work. Section (3) deals with the linearized equations of the perturbed flow. Section (4) presents the neutral curves obtained by spanning the parameter space of the problem and solving the eigenvalue/eigenfuction problem for constant and variable viscosity fluids. Conclusions are presented in Sec. (5).

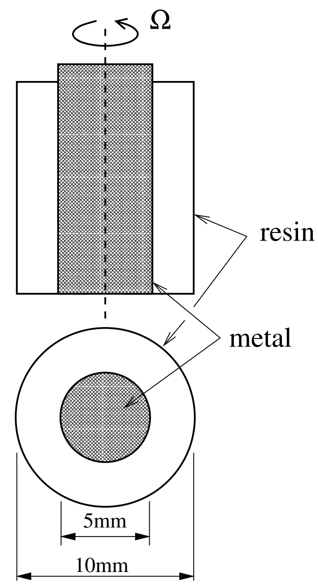

Fig. 1: The rotating disk electrode

2. The Base State

The steady hydrodynamic field is the well known Von Kármán (1921) exact solution of the continuity and Navier-Stokes equations for laminar rotating disk-flow, written in a rotating coordinate frame turning with the disk angular velocity Ω:

$$\mathbf{div}\,\mathbf{v} = 0 \tag{1}$$

$$\frac{D\mathbf{v}}{Dt} = -2\Omega \times \mathbf{v} - \frac{1}{\rho}\,\mathbf{grad}\,p + \frac{1}{\rho}\,\mathbf{div}\,\tau \tag{2}$$

where $-2\Omega \times \mathbf{v} = 2\Omega\,(v_\theta \mathbf{e}_r - v_r \mathbf{e}_\theta)$ and τ is the viscous stress tensor for a newtonian fluid with the viscosity μ depending on the axial coordinate z. The components of stress tensor are given by (Schlichting, 1968):

$$\left.\begin{aligned} \tau_{rr} &= 2\mu\frac{\partial v_r}{\partial r} & \tau_{r\theta} = \tau_{\theta r} &= \mu\left(r\frac{\partial}{\partial r}\left(\frac{v_\theta}{r}\right) + \frac{1}{r}\frac{\partial v_r}{\partial \theta}\right) \\ \tau_{\theta\theta} &= 2\mu\left(\frac{1}{r}\frac{\partial v_\theta}{\partial \theta} + \frac{v_r}{r}\right) & \tau_{\theta z} = \tau_{z\theta} &= \mu\left(\frac{\partial v_\theta}{\partial z} + \frac{1}{r}\frac{\partial v_z}{\partial \theta}\right) \\ \tau_{zz} &= 2\mu\frac{\partial v_z}{\partial z} & \tau_{rz} = \tau_{zr} &= \mu\left(\frac{\partial v_r}{\partial z} + \frac{\partial v_z}{\partial r}\right) \end{aligned}\right\} \tag{3}$$

The steady solution takes the form:

$$\bar{v}_r = r\,\Omega\,F(\xi) \tag{4}$$

$$\bar{v}_\theta = r\,\Omega\,G(\xi) \tag{5}$$

$$\bar{v}_z = (\nu(\infty)\,\Omega)^{1/2}\,H(\xi) \tag{6}$$

$$\bar{p} = \rho\nu(\infty)\Omega P(\xi) \tag{7}$$

where $\xi = z(\Omega/\nu(\infty))^{1/2}$ and $\nu(\infty)$ is the bulk viscosity, far from the electrode surface. Equations (4–7) are introduced in the dimensional continuity and Navier-Stokes equations, leading to the following system of equations for F, G, H and P.

$$2F + H' = 0 \tag{8}$$

$$F^2 - (G+1)^2 + HF' = \frac{\partial}{\partial \xi}\left(\frac{\nu(\xi)}{\nu(\infty)}F'\right) \tag{9}$$

$$2F(G+1) + HG' = \frac{\partial}{\partial \xi}\left(\frac{\nu(\xi)}{\nu(\infty)}G'\right) \tag{10}$$

$$P' + HH' = 2\frac{\nu'(\xi)}{\nu(\infty)}H' + \frac{\nu(\xi)}{\nu(\infty)}H'' \tag{11}$$

Boundary conditions for F, G and H are $F = H = P = G = 0$ when $\xi = 0$, $F = H' = 0$, $G = -1$ when $\xi \longrightarrow \infty$.In order to integrate Eqs. (8–11) a viscosity profile must be assumed. In this work we use the following profile proposed by Barcia et. al. (1992):

$$\frac{\nu(\xi)}{\nu(\infty)} = \frac{\nu(0)}{\nu(\infty)} + \left(1 - \frac{\nu(0)}{\nu(\infty)}\right)\frac{q^{1/3}}{\Gamma(4/3)}\int_0^{\xi} e^{-q\xi^3}\,d\xi \tag{12}$$

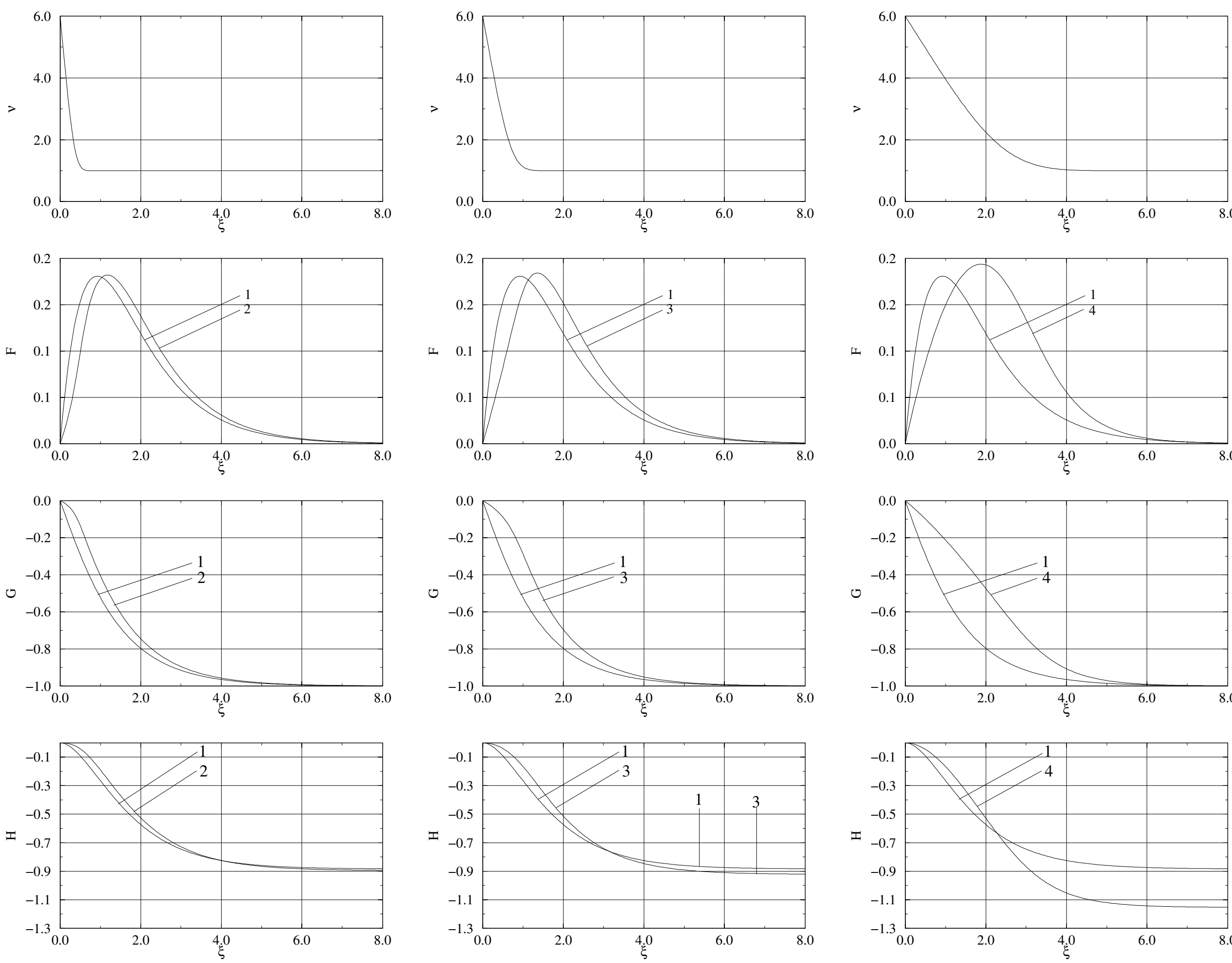

$q = 15.0$ $q = 2.00$ $q = 0.05$

Fig. 2: Dimensionless viscosity, ν, and velocity profiles F, G and H. Curves No. 1 refer to constant viscosity fluids. Curves No. 2: variable viscosity fluids with $q = 15$; Curves No. 3: $q = 2.0$; Curves No. 4: $q = 0.05$ (see Eq. 12).

Parameter q defines the slope of the viscosity profile close to the electrode surface. Fig. 1 shows the rotating disk used in the experiments conducted by our group. This electrode consists of a 5 mm diameter iron rod embedded in a 10 mm diameter epoxy resin mold such that only its bottom cross section is allowed to contact the electrolyte. Figure 2 shows the nondimensional viscosity and velocity profiles obtained by numerical integration of Eqs. (8–11) and used in the stability analysis presented in this work. Viscosity profiles with $q = 15.0$ result in a rapid decay of the viscosity to the bulk value, not changing too much the velocity profiles F, G and H. The axial component of the velocity far from the electrode is pratically the same of the case with constant viscosity and so is the incoming mass flow approaching the electrode. A decrease in the slope of the viscosity profiles obtained with $q = 2.0$ increases the deviation of the velocity profiles from the constant viscosity case. A further decrease in the value of q to 0.05 affects both the velocity profiles and the incoming mass flow rate.

3. Perturbations of the Base State

We turn now to the question of the stability of the steady configurations of the hydrodynamic field described in Sec. (2), with respect to infinitesimally small disturbances. Variables in Eqs. (1–2) are made non-dimensional as follows: radial and axial coordinates are divided the reference length $(\nu(\infty)/\Omega)^{1/2}$, velocity components are divided by the reference velocity $r_e^*\Omega$, pressure is divided by the reference pressure $\rho r_e^* \Omega^2$, viscosity is divided by the bulk value, $\nu^*(\infty)$ and time and the eigenvalue of the linearized problem are made nondimensional using the factor $\nu(\infty)^{1/2}/(r_e^*\Omega^{3/2})$. Here, r_e^* is the dimensional coordinate along the radial direction where the stability analysis is made. We define also the Reynolds number by the relation:

$$R = r_e^* \left(\frac{\Omega}{\nu(\infty)} \right)^{1/2} \tag{13}$$

The perturbed non-dimensional velocity components and pressure are written as:

$$\begin{aligned}
v_r(t,r,\theta,\xi) &= \frac{r}{R}F(\xi) + \tilde{v}_r(t,r,\theta,\xi) && (14)\\
v_\theta(t,r,\theta,\xi) &= \frac{r}{R}G(\xi) + \tilde{v}_\theta(t,r,\theta,\xi) && (15)\\
v_z(t,r,\theta,\xi) &= \frac{1}{R}H(\xi) + \tilde{v}_z(t,r,\theta,\xi) && (16)\\
p(t,r,\theta,\xi) &= \frac{1}{R^2}P(\xi) + \tilde{p}(t,r,\theta,\xi) && (17)
\end{aligned}$$

Substituting the perturbed variables given by (14–17) in the non-dimensional continuity and Navier-Stokes equations and dropping nonlinear terms we obtain:

$$\frac{\tilde{v}_r}{r} + \frac{\partial \tilde{v}_r}{\partial r} + \frac{1}{r}\frac{\partial \tilde{v}_\theta}{\partial \theta} + \frac{\partial \tilde{v}_z}{\partial \xi} = 0 \tag{18}$$

$$\begin{aligned}
&\frac{\partial \tilde{v}_r}{\partial t} + \frac{r}{R}F\frac{\partial \tilde{v}_r}{\partial r} + \frac{G}{R}\frac{\partial \tilde{v}_r}{\partial \theta} + \frac{H}{R}\frac{\partial \tilde{v}_r}{\partial \xi} + \frac{F}{R}\tilde{v}_r - \frac{2}{R}(G+1)\tilde{v}_\theta + \frac{r}{R}F'\tilde{v}_z = \\
&\quad -\frac{\partial \tilde{p}}{\partial r} + \frac{\nu}{R}\left(\frac{\partial^2 \tilde{v}_r}{\partial r^2} + \frac{1}{r^2}\frac{\partial^2 \tilde{v}_r}{\partial \theta^2} + \frac{\partial^2 \tilde{v}_r}{\partial \xi^2} + \frac{1}{r}\frac{\partial \tilde{v}_r}{\partial r} - \frac{2}{r^2}\frac{\partial \tilde{v}_\theta}{\partial \theta} - \frac{\tilde{v}_r}{r^2} \right) + \frac{\nu'}{R}\left(\frac{\partial \tilde{v}_z}{\partial r} + \frac{\partial \tilde{v}_r}{\partial \xi} \right)
\end{aligned} \tag{19}$$

$$\begin{aligned}
&\frac{\partial \tilde{v}_\theta}{\partial t} + \frac{r}{R}F\frac{\partial \tilde{v}_\theta}{\partial r} + \frac{G}{R}\frac{\partial \tilde{v}_\theta}{\partial \theta} + \frac{H}{R}\frac{\partial \tilde{v}_\theta}{\partial \xi} + \frac{F}{R}\tilde{v}_\theta + \frac{2}{R}(G+1)\tilde{v}_r + \frac{r}{R}G'\tilde{v}_z = \\
&\quad -\frac{1}{r}\frac{\partial \tilde{p}}{\partial \theta} + \frac{\nu}{R}\left(\frac{\partial^2 \tilde{v}_\theta}{\partial r^2} + \frac{1}{r^2}\frac{\partial^2 \tilde{v}_\theta}{\partial \theta^2} + \frac{\partial^2 \tilde{v}_\theta}{\partial \xi^2} + \frac{1}{r}\frac{\partial \tilde{v}_\theta}{\partial r} + \frac{2}{r^2}\frac{\partial^2 \tilde{v}_r}{\partial \theta^2} - \frac{\tilde{v}_\theta}{r^2} \right) + \frac{\nu'}{R}\left(\frac{1}{r}\frac{\partial \tilde{v}_z}{\partial \theta} + \frac{\partial \tilde{v}_\theta}{\partial \xi} \right)
\end{aligned} \tag{20}$$

$$\begin{aligned}
&\frac{\partial \tilde{v}_z}{\partial t} + \frac{r}{R}F\frac{\partial \tilde{v}_z}{\partial r} + \frac{G}{R}\frac{\partial \tilde{v}_z}{\partial \theta} + \frac{H}{R}\frac{\partial \tilde{v}_z}{\partial \xi} + \frac{H}{R}\tilde{v}_z = \\
&\quad -\frac{\partial \tilde{p}}{\partial \xi} + \frac{\nu}{R}\left(\frac{\partial^2 \tilde{v}_z}{\partial r^2} + \frac{1}{r^2}\frac{\partial^2 \tilde{v}_z}{\partial \theta^2} + \frac{\partial^2 \tilde{v}_z}{\partial \xi^2} + \frac{1}{r}\frac{\partial \tilde{v}_z}{\partial r} \right) + 2\frac{\nu'}{R}\frac{\partial \tilde{v}_z}{\partial \xi}
\end{aligned} \tag{21}$$

At this stage we assume that the perturbation variables are separable and look for a solution in the form:

$$\begin{pmatrix} \tilde{v}_r \\ \tilde{v}_\theta \\ \tilde{v}_z \\ \tilde{p} \end{pmatrix} = \begin{pmatrix} f(\xi) \\ g(\xi) \\ h(\xi) \\ \pi(\xi) \end{pmatrix} \exp[i(\alpha r + \beta R \theta - \omega t)] \tag{22}$$

where ω is a complex number, with $\Re(\omega)$ and $\Im(\omega)$ being, respectively, the frequency and the rate of growth of the perturbation. Parameters α and β are the components of the perturbation wavevector along the radial and azimutal directions. For a given time, the phase of the perturbation is constant along branches of a logarithm spiral, with the branches curved in the clockwise direction if β is positive and counter-clockwise, if negative. Substitution of the perturbation variables in Eqs. (18–21) leads to:

$$i\left(\alpha - \frac{i}{r}\right) f + i\frac{R}{r}\beta g + h' = 0 \tag{23}$$

$$i\left(\frac{r}{R}\alpha F+\beta G-\omega\right)f+\frac{r}{R}F'h+i\alpha\pi=\frac{1}{R}\left(\nu f''-\nu\left(\alpha^2+\frac{R^2}{r^2}\beta^2\right)f-Ff+2(G+1)g-\right.$$
$$\left.Hf'+i\alpha\nu'h+\nu'f'\right)+\frac{1}{R^2}\left(i\frac{R}{r}\nu\alpha f-2i\frac{R^2}{r^2}\nu\beta g\right)-\frac{\nu}{Rr^2}f \tag{24}$$
$$i\left(\frac{r}{R}\alpha F+\beta G-\omega\right)g+\frac{r}{R}G'h+i\frac{R}{r}\beta\pi=\frac{1}{R}\left(\nu g''-\nu\left(\alpha^2+\frac{R^2}{r^2}\beta^2\right)g-Fg+2(G+1)f-\right.$$
$$\left.Hg'+i\frac{R}{r}\beta\nu'h+\nu'g'\right)+\frac{1}{R^2}\left(i\frac{R}{r}\nu\alpha g-2i\frac{R^2}{r^2}\nu\beta f\right)-\frac{\nu}{Rr^2}g \tag{25}$$
$$i\left(\frac{r}{R}\alpha F+\beta G-\omega\right)h+\pi'=\frac{1}{R}\left(\nu h''-\nu\left(\alpha^2+\frac{R^2}{r^2}\beta^2\right)h-Hh'-H'h+2\nu'h'\right)+\frac{i}{Rr}\nu\alpha h \tag{26}$$

where $\lambda^2=\alpha^2+\beta^2$. Equations (23–26) show that perturbation variables are not, strictly speaking, separables. In order to overcome the problem it is necessary to make the *parallel flow* assumption, usually adopted in stability analysis of growing boundary layers, where variations of the Reynolds number in the streamwise direction are ignored. Adoption of this hypothesis in rotating disk flow (Malik,1981, 1986, Wilkinson and Malik, 1985, Lingwood, 1995) is made by replacing r by R in eqs. (23-26):

$$i\left(\alpha-\frac{i}{R}\right)f+i\beta g+h'=0 \tag{27}$$
$$i(\alpha F+\beta G-\omega)f+F'h+i\alpha\pi=\frac{1}{R}\left(\nu f''-\nu\lambda^2 f-Ff+2(G+1)g-Hf'+i\alpha\nu'h+\nu'f'\right)+$$
$$\frac{1}{R^2}\left(i\nu\alpha f-2i\nu\beta g\right)-\frac{\nu}{R^3}f \tag{28}$$
$$i(\alpha F+\beta G-\omega)g+G'h+i\beta\pi=\frac{1}{R}\left(\nu g''-\nu\lambda^2 g-Fg+2(G+1)f-Hg'+i\beta\nu'h+\nu'g'\right)+$$
$$\frac{1}{R^2}\left(i\nu\alpha g-2i\nu\beta f\right)-\frac{\nu}{R^3}g \tag{29}$$
$$i(\alpha F+\beta G-\omega)h+\pi'=\frac{1}{R}\left(\nu h''-\nu\lambda^2 h-Hh'-H'h+2\nu'h'\right)+\frac{i}{R^2}\nu\alpha h \tag{30}$$

Equations 27–30 reduce to Eqs. 2.16–2.19 given by Malik (1986), in the case of constant viscosity fluids ($\nu=1,\ \nu'=\nu''=0$).By eliminating π, neglecting terms of order R^{-2} and defining $D^n=d^n/d\xi^n$, $\bar{\alpha}=\alpha-i/R$, $\bar{\lambda}^2=\alpha\bar{\alpha}+\beta^2$ and $\eta=\alpha g-\beta f$ we obtain a sixth order system of two coupled equations in the form:

$$\left(i\nu\left(D^2-\lambda^2\right)\left(D^2-\bar{\lambda}^2\right)+i\nu'D\left(2D^2-\lambda^2-\bar{\lambda}^2\right)+i\nu''\left(D^2+\bar{\lambda}^2\right)+R\left(\alpha F+\beta G-\omega\right)\left(D^2-\bar{\lambda}^2\right)-\right.$$
$$\left.R\left(\bar{\alpha}F''+\beta G''\right)-iHD\left(D^2-\bar{\lambda}^2\right)-iH'\left(D^2-\bar{\lambda}^2\right)-iFD^2\right)h+\left(2\left(G+1\right)D+2G'\right)\eta=0 \tag{31}$$
$$\left(2\left(G+1\right)D-iR\left(\alpha G'-\beta F'\right)\right)h+\left(i\nu\left(D^2-\lambda^2\right)+i\nu'D+R\left(\alpha F+\beta G-\omega\right)-iHD-iF\right)\eta=0 \tag{32}$$

Equations 31–32 reduce to Eqs. 2.20–2.21 given by Malik (1986), in the case of constant viscosity fluids and are now rewritten in the form:

$$\begin{pmatrix} a_4D^4+a_3D^3+a_2D^2+a_1D+a_0; & b_1D+b_0 \\ c_1D+c_0; & d_2D^2+d_1D+d_0 \end{pmatrix}\begin{pmatrix} h \\ \eta \end{pmatrix}=\omega\begin{pmatrix} q_2D^2+q_0; & 0 \\ 0; & s_0 \end{pmatrix}\begin{pmatrix} h \\ \eta \end{pmatrix} \tag{33}$$

with the coefficients given by:

$$a_4=i\nu \qquad a_3=i(2\nu'-H)$$
$$a_2=i\nu''-i\nu\left(\lambda^2+\bar{\lambda}^2\right)+R\left(\alpha F+\beta G\right)-i\left(H'+F\right)$$
$$a_1=-i\nu'\left(\lambda^2+\bar{\lambda}^2\right)+iH\bar{\lambda}^2$$
$$a_0=i\bar{\lambda}^2\left(\nu''+\nu\lambda^2\right)-R\left(\alpha F+\beta G\right)\bar{\lambda}^2-R\left(\bar{\alpha}F''+\beta G''\right)+iH'\bar{\lambda}^2$$
$$b_1=2\left(G+1\right) \qquad b_0=2G'$$
$$c_1=2\left(G+1\right) \qquad c_0=-iR\left(\alpha G'-\beta F'\right)$$
$$d_2=i\nu \qquad d_1=i\left(\nu'-H\right) \qquad d_0=-i\nu\lambda^2+R\left(\alpha F+\beta G\right)-iF$$
$$q_2=R \qquad q_0=-R\bar{\lambda}^2 \qquad s_0=R$$

Eq. (33) defines a generalized eigenvalue/eigenfunction problem. The eigenfunctions are the normal modes of the model, the imaginary and real parts of each eigenvalue being, respectively, the rate of growth and the angular velocity of the perturbation relative to the angular velocity of the disk. Positive $\Re(\omega)$ mean perturbations turning angular velocity slower than the disk velocity and negative $\Re(\omega)$ mean perturbations turning faster than the disk.

For a given viscosity profile the parameter space of the problem contains *three* variables, the Reynolds number and the perturbation wavevector components α and β.

Boundary conditions of the problem require non-slip flow and vanishing axial component of the velocity at the electrode surface. These conditions are already fulfilled by the base-state, so the hydrodynamic field cannot be modified by the perturbation at the electrode surface. In consequence we must require $g = h = 0$ in $\xi = 0$. Moreover, we conclude from Eq. (23) that $h' = 0$ at the electrode surface. In $\xi \longrightarrow \infty$ we require that the perturbation vanishes ($g = h = 0$) and that $h' = 0$.

The generalized eigenvalue/eigenfunction problem is solved numerically, using the LAPACK double precision *zgegv* routine for complex generalized nonsymmetric eigenproblems.

4. Results

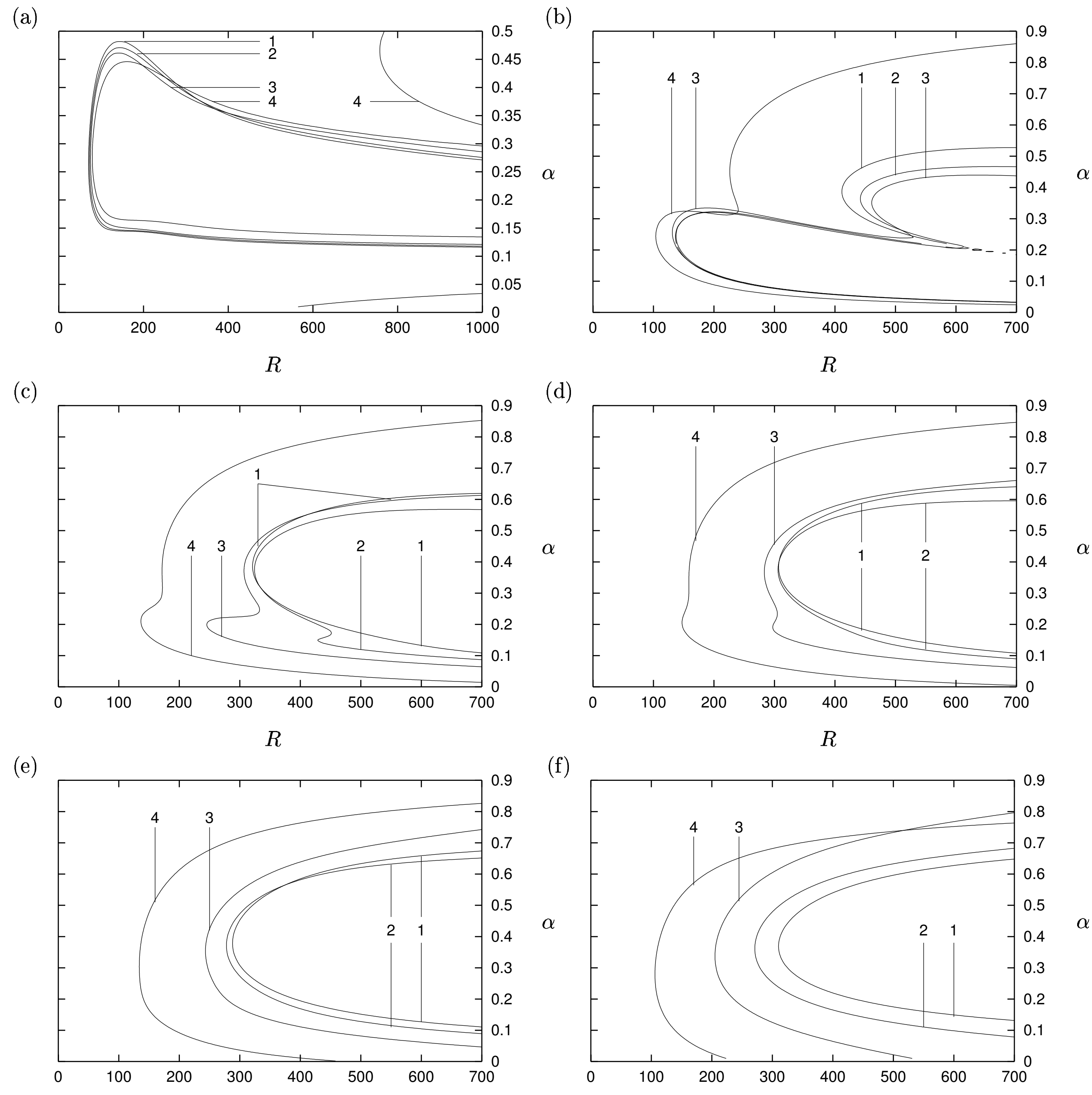

Fig. 5: Neutral curves in the plane $R \times \alpha$ for $\beta = -0.07759$ (a), $\beta = 0$ (b), $\beta = 0.03500$ (c), $\beta = 0.04672$ (d), $\beta = 0.07759$ (e) and $\beta = 0.15000$ (f). Curves No. 1 refer to constant viscosity fluids, all other, to variable viscosity fluids with $\nu(0)/\nu(\infty) = 6$. Curves No. 2: $q = 15$; Curves No. 3: $q = 2$; Curves No. 4: $q = 0.05$.

Validation of the numerical procedure used for evaluation of the neutral curves was done by comparing the coordinates of the minimum of the neutral curve presented by Malik (1986) with the results obtained with our code for constant viscosity fluids. Malik obtained for the absolute minimum of the neutral curve built for stationary disturbances, in which the real and imaginary parts of the most unstable eigenvalue vanish, the following values: $R = 285.36$, $\alpha = 0.38482$ and $\beta = 0.07759$. The values obtained with our code for the same point are $R = 286.31$, $\alpha = 0.38482$ and $\beta = 0.07753$, showing a good agreement with the literature result. Validation was done assuming a doamin with length $\xi_{max} = 30$ and a numerical grid with 601 equally spaced points. According to the validation tests we conducted this result is not significantly affected if larger domains are assumed.

In order to identify the effect of the viscosity gradient on the stability of the flow the parameter space was spanned and neutral curves associated to constant viscosity fluids and three variable viscosity profiles were evaluated. The viscosity profiles considedered were obtained with $\nu(0)/\nu(\infty) = 6$ and $q = 15$, 2 and 0.05. The resulting nondimensional viscosity and steady velocity profiles F, G and H are shown in Fig. 2. The results are presented in the form of six neutral stability diagrams, each one plotted in the $R \times \alpha$ plane, for a given value of β. These diagrams are shown in Fig. (5). Each diagram contains the neutral curve associated to constant viscosity fluids (curves No. 1) and to the three viscosity profiles considedred. Curves No. 2 refer to $q = 15$, curves No. 3, to $q = 2$ and curves No.4, to $q = 0.05$. Figures $5a - 5f$ are built for increasing values of β.

The above neutral curves show that the axial viscosity profile always changes the neutral curves from those obtained for constant viscosity fluids. The critical Reynolds number is pratically not affected by the viscosity profile in the case of $\beta = -0.3500$ but the profile has an incresing effect in the stability of the mean flow,actually reducing the flow stability, as β increases.

The neutral curves also show that the critical Reynolds number typically increases with β. The possible reason for this behaviour is that negative values of β are associated to perturbation structures turning with angular velocity sufficiently *smaller* than the disk angular velocity. As the angular velocity of the structure increases β eventually becomes positive (Faller, 1991, Lingwood, 1995). Structures turning with the disk velocity actually have $\beta > 0$ (Malik, 1986). Since lower angular velocities possibly require the transfer of smaller amounts of energy from the mean flow it seams that this is the reason why slower perturbations have a lower Reynolds number than faster ones.

In all simulations the system length was assumed as $\xi_{max} = 10$ and the eigenvalue/eigenvector problem was solved in the nodes of a grid containing 201 uniformly spaced points. This length is not large enough to assure convergence of the neutral curves to sets of points independent of the system length, so it is expected that the curves may quantitatively change if larger system are assumed. However, we believe that the main result given in this paper – that an axial viscosity profile changes the neutral curves, and leads to less stable flows in most cases, will not be affected by a more precise evaluation of the neutral curves.

5. Conclusions

In conclusion we studied the stability of rotating disk flows in electrochemical cells, where the fluid viscosity varies along the axis of the rotating electrode and presented the linear equations governing the evolution of spiral perturbations imposed to the steady flow. These equations reduce to those presentd by Malik (1986) in the case of constant viscosity fluids. Comparison of our results for constant viscosity flows, concecrning the coordinates of the miniumum of the neutral curve for stationary disturbances with results existing in the literature indicate good agreement and provide validation of our numerical code.

Variable viscosity neutral curves, drawn for fixed values of parameter β, indicate that axial viscosty profiles significantly affect the neutral stability curves. Neutral curves associated to a wide range of values of β become more unstable if varaible viscosity is assumed. It is interesting to remark that in these cases the flow becomes less stable with an increase in the fluid viscosity close to the disk surface. This decrease of stability is possibly due to the changes introduced in the base state by the viscosity profile.

The results presented suport the hypothesis that the current oscillations observed in the polarization curve may originate from a hydrodynamic instability, since the neutral curves presented in this work for variable viscosity fluids show that the crititical Reynolds number can be reduced to less than 50% of the value obtained for constant viscosity fluids.

Next stages of the present study will include the evaluation of the neurtral curves for disturbances turning with specified angular velocity, as presented by Faller (1991) and Lingwood (1995), as opposed to the curves with specified β, presented in this paper.

6. Acknowledgements

The numerical calculations were done at the High-Performance Computer Center (NACAD-UFRJ) and in the workstations of the Metallurgy and Materials Eng. Dept. (UFRJ). The authors acknowledge fruitfull discussions with profs. R. E. Kelly from the University of California at Los Angeles and D. Walgraef from the Free Unversity of Brussels.

7. References

Anderson, E., Bai, Z., Bischof, C., Demmel, J., Dongorra, J., Croz, J. D., Greenbaum, A., Hammarling, S., McKenney, A., Ostrouchov, S., and Sorensen, D., 1995, "LAPACK User's Guide", SIAM, Philadelphia, USA.

Barcia, O. E., Mattos, O. R., and Tribollet, B., 1992, Anodic dissolution of iron in acid sulfate under mass transport control, "J. Eletrochem. Soc.", Vol. 139, pp. 446–453.

Epelboin, I., Gabrielli, G., Keddam, M., Lestrach, J. C., and Takenouti, H., 1979, Passivation of Iron in Sulfuric acid Medium, "J. Eletrochem. Soc.", Vol. 126, pp. 1632–1637.

Faller, A. J., 1991, Instability and Transition of the Disturbed Flow Over a Rotating Disk, "J. Fluid Mech.", Vol. 230, pp. 245–269.

Ferreira, J. R. R. M., Barcia, O. E., and Tribollet, B., 1994, Iron dissolution under mass transport control: the effect of viscosity on the current oscillation, "Eletrochim. Acta", Vol. 39, pp. 933–938.

Lingwood, R. J., 1995, Absolute instability of the boundary layer on a rotating disk, "J. Fluid Mech.", Vol. 299, pp. 17–33.

Malik, M. R., 1986, The Neutral Curve for Stationary Disturbances in Rotating-disk Flow, "J. Fluid Mech.", Vol. 164, pp. 275–287.

Malik, M. R., Wilkinson, and Orzag, S. A., 1981, Instability and Transition in a Rotating Disk, "AIAA J.", Vol. 19-9, pp. 1131–1138.

Pontes, J., Mangiavacchi, N., Conceição, A. R., Barcia, O. E., Mattos, O. E., and Tribollet, B., to appear, Instabilities in Electrtochemical Systems with a Rotatinng Disk electrode, "J. of the Braz. Soc. of Mechanical Sciences", Vol. .

Schlichting, H., 1968, "Boundary Layer Theory", McGraw-Hill.

von Kármán, T. and Angew, Z., 1921, Uber Laminare und Turbulente Reibung, "Math. Mec.", Vol. 1, pp. 233–252.

Wilkinson, s. and R., M. M., 1985, Stability Experiments in the Flow Over a Rotating Disk, "AIAA J.", Vol. 23, pp. 588.